7-2017

Infrared Multiple-Photon Dissociation Action Spectroscopy of the b(2)(+) Ion from PPG: Evidence of Third Residue Affecting b(2)(+) Fragment Structure

John C. Poutsma
College of William and Mary, jcpout@wm.edu

Jonathan Martens

Jos Oomens

Phillipe Maitre

Vincent Steinmetz

See next page for additional authors

Recommended Citation

Poutsma, John C.; Martens, Jonathan; Oomens, Jos; Maitre, Phillipe; Steinmetz, Vincent; Bernier, Matthew; Jia, Mengxuan; and Wysocki, Vicki, Infrared Multiple-Photon Dissociation Action Spectroscopy of the b(2)(+) Ion from PPG: Evidence of Third Residue Affecting b(2)(+) Fragment Structure (2017). *JOURNAL OF THE AMERICAN SOCIETY FOR MASS SPECTROMETRY*, 28(7). 10.1007/s13361-017-1659-2

Published in final edited form as:

J Am Soc Mass Spectrom. 2017 July ; 28(7): 1482–1488. doi:10.1007/s13361-017-1659-2.

Infrared Multiple-photon Dissociation Action Spectroscopy of the b_2^+ ion from PPG: Evidence of third residue affecting b_2^+ fragment structure

John C. Poutsma[1], **Jonathan Martens**[2], **Jos Oomens**[2,3], **Phillipe Maitre**[4], **Vincent Steinmetz**[4], **Matthew Bernier**[5], **Mengxuan Jia**[5], and **Vicki Wysocki**[5]

[1]Department of Chemistry, The College of William and Mary, Williamsburg, VA 23187 [2]Radboud University, Institute for Molecules and Materials, FELIX Laboratory, Toernooiveld 7c, NL-6525ED Nijmegen, The Netherlands [3]Van 't Hoff Institute for Molecular Sciences, University of Amsterdam, Science Park 908, 1098XH Amsterdam, The Netherlands [4]Laboratoire de Chimie Physique, CNRS UMR 8000, Université Paris Sud, Université Paris Saclay, CNRS, Orsay, France [5]Department of Chemistry, Ohio State University, Columbus, OH, 43210 USA

Abstract

Infrared multiple-photon dissociation (IRMPD) action spectroscopy was performed on the b_2^+ fragment ion from the protonated PPG tripeptide. Comparison of the experimental infrared spectrum with computed spectra for both oxazolone and diketopiperazine structures indicates that the majority of the fragment ion population has an oxazolone structure with the remainder having a diketopiperazine structure. This result is in contrast with a recent study of the IRMPD action spectrum of the PP b_2^+ fragment ion from PPP, which was found to be nearly 100% diketopiperazine (Martens et al. *Int. J. Mass Spectrom*. **2015**, *377*, 179). The diketopiperazine b_2^+ ion is thermodynamically more stable than the oxazolone but normally requires a *trans/cis* peptide bond isomerization in the dissociating peptide. Martens et al. showed through IRMPD action spectroscopy that the PPP precursor ion was in a conformation in which the first peptide bond is already in the *cis* conformation and thus it was energetically favorable to form the thermodynamically-favored diketopiperazine b_2^+ ion. In the present case, solution-phase NMR spectroscopy and gas-phase IRMPD action spectroscopy shows that the PPG precursor ion has its first amide bond in a *trans* configuration suggesting that the third residue is playing an important role in both the structure of the peptide and the associated ring-closure barriers for oxazolone and diketopiperazine formation.

Introduction

With the reliance on mass spectrometry-based proteomics in the identification of proteins in biological research, the gas-phase fundamentals of peptide sequencing are of major importance. Even with the development of increasingly more sophisticated software and instrumentation that has made data collection and processing simpler and more reliable,

Correspondence to: John C. Poutsma; Vicki Wysocki.

protein sequence coverage is still greatly affected by the presence or lack of specific amino acid residues or combinations of residues within a protein. [1] Much of the work that has been focused on improving algorithms has made use of specific amino acid sequence trends [2] that are still not fully understood. In order to further these pursuits there must be explanations as to the underlying fundamentals of peptide fragmentation mechanisms and how specific residues may guide protein coverage challenges.

Collision-induced dissociation produces fragments that form *via* cleavage at the C-N peptide bond along the peptide backbone, where charge can either be retained on the C-terminus to form a y-ion or N-terminally to produce a b-ion.[3,4] One focus in peptide fragmentation and the underlying mechanisms has centered on the b_2^+ ion, as its structure is directly tied to the conformation of the peptide backbone of the precursor peptide. Fragmentation may lead to either a five-membered oxazolone ring, which retains a *trans* conformation at the peptide bond, or a diketopiperazine six-membered ring structure, which can only form via *trans-cis* isomerization of the peptide bond.[5,6] For most amino acid sequences, the most common structure formed for the b_2^+ ion is the oxazolone despite the fact that the diketopiperazine is typically found to be more thermodynamically stable. The thermodynamic preference for *trans*-amide bonds in peptides is thought to be a contributing factor for this finding. The difference in ring closure barriers for the formation of oxazolone and diketopiperazine is also likely playing a role in the prevalence of the oxazolone.[7,8]

Proline is well known to significantly affect the secondary structure of peptide and proteins and the fragmentation of any peptide in which it resides leading to the “proline effect”,[9–11] which is preferential cleavage of the peptide bond N-terminal to the proline resulting in enhanced intensity of the corresponding y-ion due in part to the increased proton affinity of the secondary amine proline.[12,13] Consequently, proline has been part of many peptide fragmentation model studies. Proline-containing peptides have been shown to have a higher propensity for forming *cis* peptide bonds at the Pro residue as its barrier to *trans/cis* isomerization of the N-terminally adjacent peptide bond is ~55 kJ/mol compared to the average ~80 kJ/mol for the other 19 protein amino acids.[14] The difference in energy between the *trans* and *cis* isomers of proline-containing peptides is also 8 kJ/mol smaller than the difference for other residues.[15] Consequently, the diketopiperazine b_2^+ ion is observed at greater frequency in model peptides that contain proline in the second position presumably because formation of the *cis*-peptide bond required to facilitate head-to-tail cyclization is significantly easier with proline in this position. In previous research, Gucinski *et al.* observed mixtures of oxazolone and diketopiperazine in the b_2^+ ion structures of Val-Pro, Ala-Pro, and Ile-Pro and only the diketopiperazine structure for His-Pro, which stressed the importance of the *trans/cis* isomerization barrier in the formation of the diketopiperazine and explained that for His-Pro there was a combined effect of the basic imidazole residue from the histidine in the first position and the second position proline contributing to the stability of the *cis*-form of the peptide.[16]

Recent efforts have also dealt with the peptide fragments formed from proline at different positions within the peptide backbone and the ways that multiple proline residues within a peptide can affect their precursor and fragment structures.[13,17–20] In analysis of precursor peptides containing proline, Masson et al., using both spectroscopy and ion

mobility, confirmed that GPGG was comprised of a larger kinetically trapped *trans*-Pro population and a smaller *cis*-Pro population that was found to be more thermodynamically stable in the gas-phase. [21]

While much of the work from previous studies has focused on the effect of the second position proline and the effect of single proline residues within a peptide, polyproline has also been an important biologically relevant sequence feature, most notably due to its presence in collagen and in structural motifs of proteins such as beta-helices.[22–24] Likewise, polyproline chains, which have been extensively studied both in solution and the gas phase for their structural effects, have been observed for their influence in the formation of b-ion structures.[25] Most recently Martens *et al.*[26] have examined the fragment ions of small polyproline chains from the tripeptide to hexapeptide. IRMPD action spectroscopy was used to confirm ion mobility and modeling studies that found that small polyproline peptides adopt structures with the first amide bond in the *cis* configuration and the remaining amide bonds in either *cis* or *trans* configuration. [22] For the PPP tripeptide, this study found the resulting b_2^+ ion to exist as exclusively a diketopiperazine with the IRMPD action spectrum of the precursor tripeptide most closely matching that of the cis-cis conformation for the two peptide bonds within the peptide.

In this work, we follow up the work from the polyproline PPP and compare the results to the tripeptide PPG, which is most relevantly found as part of the sequence of bradykinin, and serves to compare the influence of the third residue on the resulting b_2^+ ion structure. As with the previous experiments performed on polyproline, ion structures were determined via IRMPD action spectroscopy and were compared to DFT calculations. Once again, the *cis/trans* nature of the amide bonds within the precursor tripeptide are of critical importance in addressing the nature of the b_2^+ ion structure and from this experiment direct comparisons can be made on the influence of the third residue.

Experimental and Theoretical Methods

Infrared multiphoton dissociation spectra were obtained at the Free Electron Laser for Infrared eXperiments (FELIX) [27,28] facility in Nijmegen, Netherlands and at the Centre Laser Infrarouge d'Orsay in Orsay, France.[29,30]

a. FELIX

A dilute solution (0.1 μM) of PPG in slightly acidified acetonitrile (0.1% formic acid) was directly infused into a modified Bruker Amazon ion trap mass spectrometer coupled to the FELIX beamline. The protonated peptide precursor ions $[M+H]^+$ (m/z 270) were generated from electrospray ionization, mass isolated and allowed to undergo collision-induced dissociation (CID) with the background helium gas at a collision energy chosen to optimize the formation of the b_2^+ product ion. A representative collision-induced dissociation spectrum for PPG+H^+ is shown in Figure S1 of Supporting Information. As shown in the spectrum, the major fragment is the "proline effect" y_2^+ ion at m/z 173, but there was sufficient intensity of the b_2^+ ion at m/z 195 for IRMPD action spectroscopy studies. The PP b_2^+ fragment ions are re-isolated and then irradiated with infrared radiation from 900 to 2000 cm^{-1} from the free-electron laser. The infrared radiation comes in 5 μs macro-pulses

with an approximate energy of 30–40 mJ/pulse and a bandwidth of 0.4% of the center frequency. IRMPD action spectroscopy of the b_2^+ ion gives an a_2^+ fragment at m/z 167 and three internal proline-derived ions at m/z 126, 98, and 70. An IRMPD action spectrum for b_2^+ is generated by plotting the dissociation yield for product ion formation Σ (product ions)/Σ (product ions + un-reacted precursor) as a function of wavelength. The wavelength scale is calibrated using a grating spectrometer and the dissociation yield is linearly corrected for variations in laser power.

b. CLIO

Similar procedures were employed to obtain IRMPD action spectra at the CLIO facility. A dilute solution (10 μM) of PPG in slightly acidified acetonitrile (0.1% formic acid) was directly infused into a modified Bruker Esquire ion trap mass spectrometer coupled to the CLIO free electron laser source. Parent ion isolation, collision-induced dissociation, and b_2^+ product re-isolation procedures are the same as those in the FELIX laboratory. The collision-induced dissociation spectrum (not shown) for PPG+H^+ was virtually identical to the spectrum obtained at FELIX, with a dominant y_2^+ "proline effect" fragment ion and a minor b_2^+ ion. The collision energy was varying in order to maximize the intensity of b_2+. The FEL output consists of 8 μs macropulses at 25 Hz. The macropulse energy is *ca.* 20 mJ. The laser wavelength is varied in *ca.* 6 cm^{-1} steps and the laser bandwidth is about 0.3–0.5% of the center wavelength. IRMPD action spectroscopy of the b_2^+ ion gives the same four fragment ions as found in FELIX. The wavelength scale is calibrated by passing part of the beam through a polystyrene film and comparing peaks to the known IR spectrum in the region between 1000 and 2000 cm^{-1}. The dissociation yield is linearly corrected for variations in laser power.

c. Theoretical methods

Low energy conformations for the PPG+H^+ precursor, and both the protonated oxazolone and protonated diketopiperazine forms of PP b_2^+ were generated using the GMMX conformer searching routine in PCModel 9.3. All conformers within 60 kJ/mol of the global minimum structure were kept. Unique conformers from the GMMX search were used as starting structures for increasingly larger calculations. Geometries, zero-point energies, enthalpy- and free-energy-corrections, and harmonic vibrational frequencies were ultimately calculated at the B3LYP/6-31+G(d,p) level of theory. Single-point energies at the B3LYP/6-311++G(d,p) level of theory were carried out at the double zeta geometry. Harmonic vibrational frequencies for PP b_2^+ were scaled by 0.965 and those for PPG+H^+ were scaled by 0.970. Stick spectra were broadened by a 20 cm^{-1} baseline-width Gaussian function.

Results and Discussion

Collision-induced dissociation of the protonated peptide [PPG+H^+] gives a peak with m/z 195 that corresponds to b_2^+. This fragment ion was isolated and allowed to interact with tunable infrared radiation from the FEL. IRMPD action spectra for PP b_2^+ ion from CLIO and FELIX are shown in Figure 1a and 1b, respectively and clearly show an intense peak near 1925 cm^{-1} that is diagnostic for an oxazolone structure.[31,32] Computed infrared spectra for the lowest energy oxazolone and diketopiperazine conformers are also shown in

Figure 1c and 1d, respectively. Additional peaks in the experimental spectrum near 1600, 1282, and 1100 cm^{-1} also match the oxazolone spectrum. Smaller peaks near 1630 (CLIO), 1700, and 1400 cm^{-1} indicate that the gas-phase ion population contains a small amount of the diketopiperazine isomer as well.

Table S1 shows the relative energetics of the eight diketopiperazine structures and six oxazolone conformers found in the conformational search. The conformer with the lowest free-energy for PP b_2^+ is a diketopiperazine and is shown in Figure 2. It has both proline rings puckered in the same direction and the ionizing proton *anti* to the ring nitrogen. Higher energy conformers arise from different ring puckering schemes and/or a *syn* arrangement for the ionizing proton with respect to the ring nitrogen atom (Figure 2). The different ring puckering schemes have a modest effect on the computed spectra in this region, whereas a *syn* arrangement for the ionizing proton with respect to the ring nitrogen atom shifts the peak near 1682 cm^{-1} to the red. For comparison, the computed spectrum of the lowest-energy conformer with a *syn*-OH is also shown in Figure 1e. The four diketopiperazine conformers with the lowest free energies should account for > 95% of the diketopiperazine population at 298K.

The lowest energy protonated oxazolone structure lies *ca.* 70 kJ/mol higher in energy than the lowest energy diketopiperazine and is shown in Figure 3. Due to the cyclic side chain of proline, the oxazolone structure is bicyclic and contains a formally positive nitrogen atom in the ring system. Higher energy conformers arise from different orientations of the external proline ring with respect to the oxazolone rings as well as from differences in the proline ring puckering. The conformers with the two lowest free energies should constitute > 95% of the oxazolone Boltzmann population at 298 K. The diagnostic oxazolone peaks near 1925 and 1600 cm^{-1} are in virtually the same position for both of these conformers.

It is clear from the experimental spectra (Figures 1a and 1b) that the majority of the conformers under both of our experimental conditions are oxazolones. This result is in stark contrast with previous results for the PP b_2^+ fragment ion from PPP that was shown to be nearly 100% diketopiperazine.[26] In that study the protonated [PPP+H^+] precursor was found to be in the *cis/cis* configuration, which is primed for diketopiperazine formation. A collision-induced dissociation spectrum for PPP+H^+ is shown in Figure S2 of Supporting Information. As with PPG+H^+, the dominant fragment ion is the “proline” effect y_2^+ ion. In this case, the b_2^+ is more intense than in PPG+H^+ and is of ample intensity for further IRMPD action spectroscopy studies.

In order to ascertain the conformation of the PPG+H^+ precursor peptides, we obtained a solution-phase (50% D_2O:50% CD_3CN) NMR spectrum of the neutral PPG peptide. The spectrum is shown in Figure S3 of Supporting Information. Analysis of the C_α hydrogens indicates that the neutral peptide is a mixture of isomers, with the dominant structure being the *trans/trans* isomer (*ca.* 5:1 of *trans/trans*: *trans:cis*). Peaks were assigned based on 1D-selective TOCSY experiments, and the conformations were established on the basis of 1D-selective NOESY experiments.[33,34] We were also able to obtain the gas-phase IRMPD action spectrum of PPG+H^+ precursor ion at the FELIX facility as shown in Figure 4. Also shown in Figure 4 are calculated scaled harmonic spectra at the B3LYP/6-31+G(d,p) level of

theory for the lowest free energy conformers of the 4 different isomers of PPG+H^+ (*cis/trans, trans/trans, cis/cis*, and *trans/cis*). Figure 5 shows the lowest energy conformers for these isomers and Table S2 gives relative 298K free energy values at the B3LYP/6-311++G(d,p)//B3LYP/6-31+G(d) for all isomers found in our conformational search. The calculations predict that the lowest-energy isomer is *cis/trans*, with *trans/trans* isomers lying on the order of 13 kJ/mol higher in energy. The lowest energy *cis/cis* and *trans/cis* structures are on the order of 25 and 32 kJ/mol higher in energy at the B3LYP/6-31+G(d,) level of theory.

An analysis of the IRMPD action spectrum shows that the experimental spectrum matches best with the *trans/trans* isomer which means that the much of the gas-phase peptide population is being kinetically trapped in the favored solution-phase structure during the electrospray process. Given the intensity of the peak in the experimental spectrum near 1505 cm^{-1} we can conclude that the gas-phase sample does not contain significant amounts of *trans/cis* or *cis/cis* isomers as the calculated spectra have not significant peaks in this region of the spectrum. Thus the minor isomer in solution is absent from the spectrum. Additionally, the intensity in the experimental spectrum around 1730 cm^{-1} indicates that the *cis*/*trans* isomer is present in the sample as at least a minor component. The fact that the b_2^+ ion population contains mostly oxazolone with a small amount of diketopiperazine is consistent with a precursor mixture of mostly *trans/trans* (giving the oxazolone) with a sub-population of *cis/trans* PPG+H^+ precursor (giving the diketopiperazine). An alternative explanation for the b_2^+ structure distribution is that the barrier to *trans/cis* isomerization is below that of either of the ring-closure barriers for product formation and that the distribution arises from the Curtin-Hammet principle.[35,36] This mechanism would be in agreement with calculations by Armentrout [8] on protonated diglycine that show that the rate limiting step is ring closure to the final product and with experimental data of Morrison and Wysocki [37] that show that the third residue of a peptide can dramatically influence the b_2^+ structure. A full computational study for these peptides and those containing dimethylproline, which locks peptide bonds into *cis* conformations, including the calculation of the relevant barrier heights for *trans-cis* isomerization and product formation is underway.

Conclusions

Collision-induced dissociation of protonated PPG tripeptide gives a mixture of b_2^+ ions that are predominantly oxazolone. This is in contrast with the population of b_2^+ ions from CID of protonated PPP. Clearly, the fragmentation mechanism for b_2^+ ion formation from small peptides depends not only on the first two residues that make up the nascent b_2^+ ion but also on the identity of trailing residues that affect the structure of the peptide and the relevant barriers for dissociation.

Supplementary Material

Refer to Web version on PubMed Central for supplementary material.

Acknowledgments

This work was supported by the National Science Foundation, JCP: (CHEM:1464763), the National Institutes of Health, JCP (1R15GM116180-01), and the Ohio State University Eminent Scholar Funds. The authors acknowledge the excellent assistance from the FELIX and CLIO operators and staff. J.M. and J.O. are in part financially supported by NWO Chemical Sciences under VICI project nr. 724.011.002. The authors also wish to thank the Ohio State NMR Facility for obtaining and analyzing the PPG NMR spectrum.

References

1. Breci LA, Tabb DL, Yates JR 3rd, Wysocki VH. Cleavage N-terminal to proline: analysis of a database of peptide tandem mass spectra. Anal Chem. 2003; 75:1963. [PubMed: 12720328]
2. Li W, Ji L, Goya J, Tan G, Wysocki VH. SQID: an intensity-incorporated protein identification algorithm for tandem mass spectrometry. J Proteome Res. 2011; 10:1593. [PubMed: 21204564]
3. Yalcin T, Khouw C, Csizmadia IG, Peterson MR, Harrison AG. Why are B ions stable species in peptide spectra? J Am Soc Mass Spectrom. 1995; 6:1165. [PubMed: 24214067]
4. Paizs B, Suhai S. Fragmentation pathways of protonated peptides. Mass Spectrom Rev. 2005; 24:508. [PubMed: 15389847]
5. Harrison AG, Csizmadia IG, Tang TH. Structure and fragmentation of b2 ions in peptide mass spectra. J Am Soc Mass Spectrom. 2000; 11:427. [PubMed: 10790847]
6. Grewal RN, El Aribi H, Harrison AG, Siu KWM, Hopkinson AC. Fragmentation of Protonated Tripeptides: The Proline Effect Revisited. J Phys Chem B. 2004; 108:4899.
7. Balta B, Aviyente V, Lifshitz C. Elimination of water from the carboxyl group of GlyGlyH+ J Am Soc Mass Spectrom. 2003; 14:1192. [PubMed: 14530099]
8. Armentrout PB, Heaton AL. Thermodynamics and mechanisms of protonated diglycine decomposition: a computational study. J Am Soc Mass Spectrom. 2012; 23:621. [PubMed: 21952767]
9. Schwartz BL, Bursey MM. Some Proline Substituent Effects in the Tandem Mass Spectrum of Protonated Pentaalanine. Biol Mass Spectrom. 1992; 21:92. [PubMed: 1606186]
10. Loo JA, Edmonds CA, Smith RD. Tandem Mass Spectrometry of Very Large Molecules. 2. Dissociation of Multiply Charged Proline-Containing Proteins from Electrospray Ionization. Anal Chem. 1993; 65:425. [PubMed: 8382455]
11. Vaisar T, Urban J. Probing the Proline Effect in CID of Protonated Peptides. J Mass Spectrom. 1996; 31:1185. [PubMed: 8916427]
12. Bleiholder C, Suhai S, Harrison AG, Paizs B. Towards understanding the tandem mass spectra of protonated oligopeptides. 2: The proline effect in collision-induced dissociation of protonated Ala-Ala-Xxx-Pro-Ala (Xxx = Ala, Ser, Leu, Val, Phe, and Trp). J Am Soc Mass Spectrom. 2011; 22:1032. [PubMed: 21953044]
13. Raulfs MDM, Breci L, Bernier M, Hamdy OM, Janiga A, Wysocki V, Poutsma JC. Investigations of the mechanism of the Proline Effect“ in tandem mass spectrometry experiments: The “Pipecolic Acid Effect”. J Am Soc Mass Spectrom. 2014; 25:1705. [PubMed: 25078156]
14. Pal D, Chakrabarti P. Cis Peptide Bonds in Proteins: Residues Involved, their Conformations, Interactions and Locations. J Mol Biol. 1999; 294:271. [PubMed: 10556045]
15. Jorgensen WL, Gao J. Cis Trans Energy Difference for the Peptide-Bond in the Gas-Phase and in Aqueous-Solution. Journal of the American Chemical Society. 1988; 110:4212.
16. Gucinski AC, Chamot-Rooke J, Steinmetz V, Somogyi A, Wysocki VH. Influence of N-terminal residue composition on the structure of proline-containing b2+ ions. J Phys Chem A. 2013; 117:1291. [PubMed: 23312013]
17. Thomas KM, Naduthambi D, Zondlo NJ. Electronic control of amide cis-trans isomerism via the aromatic-prolyl interaction. J Am Chem Soc. 2006; 128:2216. [PubMed: 16478167]
18. Smith LL, Herrmann KA, Wysocki VH. Investigation of gas phase ion structure for proline-containing b(2) ion. J Am Soc Mass Spectrom. 2006; 17:20. [PubMed: 16338148]

19. Knapp-Mohammady M, Young AB, Paizs B, Harrison AG. Fragmentation of doubly-protonated Pro-His-Xaa tripeptides: formation of b(2)(2+) ions. J Am Soc Mass Spectrom. 2009; 20:2135. [PubMed: 19683937]
20. Bleiholder C, Suhai S, Harrison AG, Paizs B. Towards Understanding the Tandem Mass Spectra of Protonated Oligopeptides. 2: The Proline Effect in Collision-induced Dissociation of Protonated Ala-Ala-Xxx-Pro-Ala (Xxx = Ala, Ser, Leu, Val, Phe, and Trp). J Am Soc Mass Spectrom. 2011; 21:1032.
21. Masson A, Kamrath MZ, Perez MA, Glover MS, Rothlisberger U, Clemmer DE, Rizzo TR. Infrared Spectroscopy of Mobility-Selected H+-Gly-Pro-Gly-Gly (GPGG). J Am Soc Mass Spectrom. 2015; 26:1444. [PubMed: 26091889]
22. Counterman AE, Clemmer DE. Anhydrous Polyproline Helices and Globules. J Phys Chem B. 2004; 108:4885.
23. Avenoza A, Busto JH, Cativiela C, Peregrina JM, Rodriguez F. β-Turn modulation by the incorporation of c6Ser into Xaa-Pro dipeptide. Tetrahedron Lett. 2002; 43:1429.
24. Moradi M, Babin V, Roland C, Darden TA, Sagui C. Conformations and free energy landscapes of polyproline peptides. Proc Natl Acad Sci U S A. 2009; 106:20746. [PubMed: 19923435]
25. Unnithan AG, Myer MJ, Veale CJ, Danell AS. MS/MS of Protonated Polyproline Peptides: The Influence of N-terminal Protonation on Dissociation. J Am Soc Mass Spectrom. 2007; 18:2198. [PubMed: 17964801]
26. Martens JK, Grzetic J, Berden G, Oomens J. Gas-phase conformations of small polyprolines and their fragment ions by IRMPD spectroscopy. Int J Mass Spectrom. 2015; 377:179.
27. Martens J, Grzetic J, Berden G, Oomens J. Structural identification of electron transfer dissociation products in mass spectrometry using infrared ion spectroscopy. Nat Commun. 2016; 7:11754. [PubMed: 27277826]
28. Martens JK, Berden G, Gebhardt CR, Oomens J. Infrared ion spectroscopy in a nodified quadrupole ion trap mass spectrometer at the FELIX free electron laser laboratory. Rev Sci Instrum. 2016; 87doi: 10.1063/1.4964703
29. Prazeres R, Glotin F, Insa C, Jaroszynski DA, Ortega JM. Two-colour operation of a Free-Electron Laser and applications in the mid-infrared. Eur J Mass Spectrom. 1998; 3:87.
30. Aleese LM, Simon A, McMahon TB, Ortega JM, Scuderi D, Lemaire J, Maitre P. Mid-IR spectroscopy of protonated leucine methyl ester performed with an FTICR or a Paul type ion-trap. Int J Mass Spectrom. 2006; 249:14.
31. Polfer NC, Oomens J, Suhai S, Paizs B. Spectroscopic and Theoretical Evidence for Oxazolone Ring Formation in Collision-Induced Dissociation of Peptides. J Am Chem Soc. 2005; 127:17154. [PubMed: 16332041]
32. Yoon SH, Chamot-Rooke J, Perkins BR, Hilderbrand AE, Poutsma JC, Wysocki VH. IRMPD Spectroscopy Shows That AGG Forms an Oxazolone b2+ Ion. J Am Chem Soc. 2008; 130:17644. [PubMed: 19061412]
33. Stott K, Stonehouse J, Keeler J, Hwang TL, Shaka AJ. Excitation Sculpting in High-Resolution Nuclear Magnetic Resonance Spectroscopy: Application to Selective NOE Experiments. J Am Chem Soc. 1995; 117:4199.
34. Thrippleton MJ, Keeler J. Elimination of Zero-Quantum Interference in Two-Dimensional NMR Spectra. Angew Chem, Int Ed. 2003; 42:3938.
35. Haupert LJ, Poutsma JC, Wenthold PG. The Curtin-Hammett Principle in Mass Spectrometry. Acc Chem Res. 2009; 42:1480. [PubMed: 19572743]
36. Curtin DY. Stereochemical Control of Organic Reactions. Differences in Behavior of Diastereomers 1. Ethane Derivatives. The cis effect. Rec Chem Prog. 1954; 15:111.
37. Morrison LJ, Chamot-Rooke J, Wysocki VH. IR action spectroscopy shows competitive oxazolone and diketopiperazine formation in peptides depends on peptide length and identity of terminal residue in the departing fragment. Analyst. 2014; 139:2137. [PubMed: 24618890]

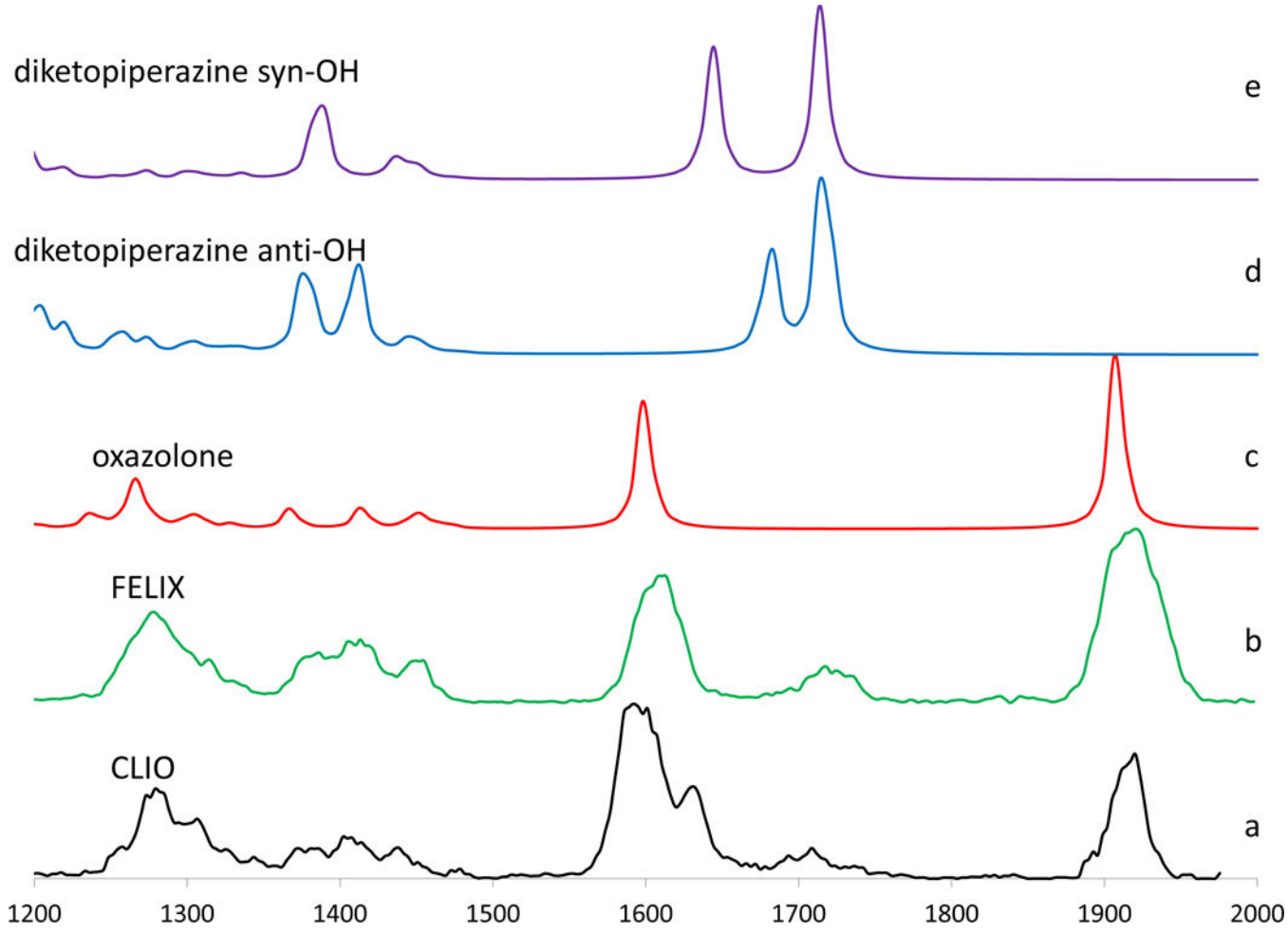

Figure 1.

Experimental IRMPD action spectrum for b_2^+ ion from PPG obtained at a) CLIO facility and b) FELIX. Computed spectra for c) lowest energy oxazolone conformer, d) lowest energy diketopiperazine structure with *anti*-OH, and e) lowest energy diketopiperazine structure with *syn*-OH.

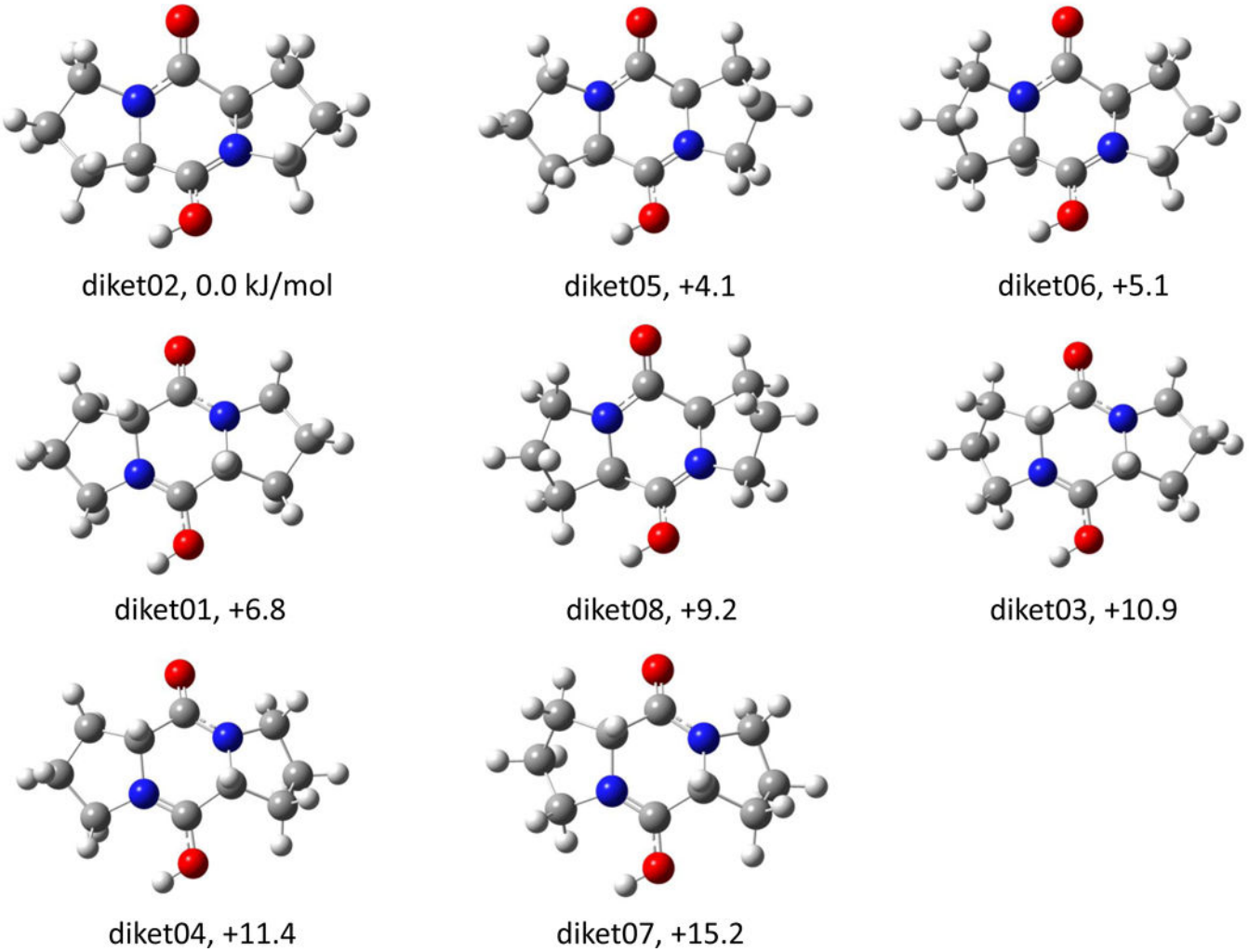

Figure 2.

Low-energy conformers for diketopiperazine PP b_2^+ ions. Numbers are ΔG values in kJ/mol at 298 K relative to the lowest energy diketopiperazine conformer.

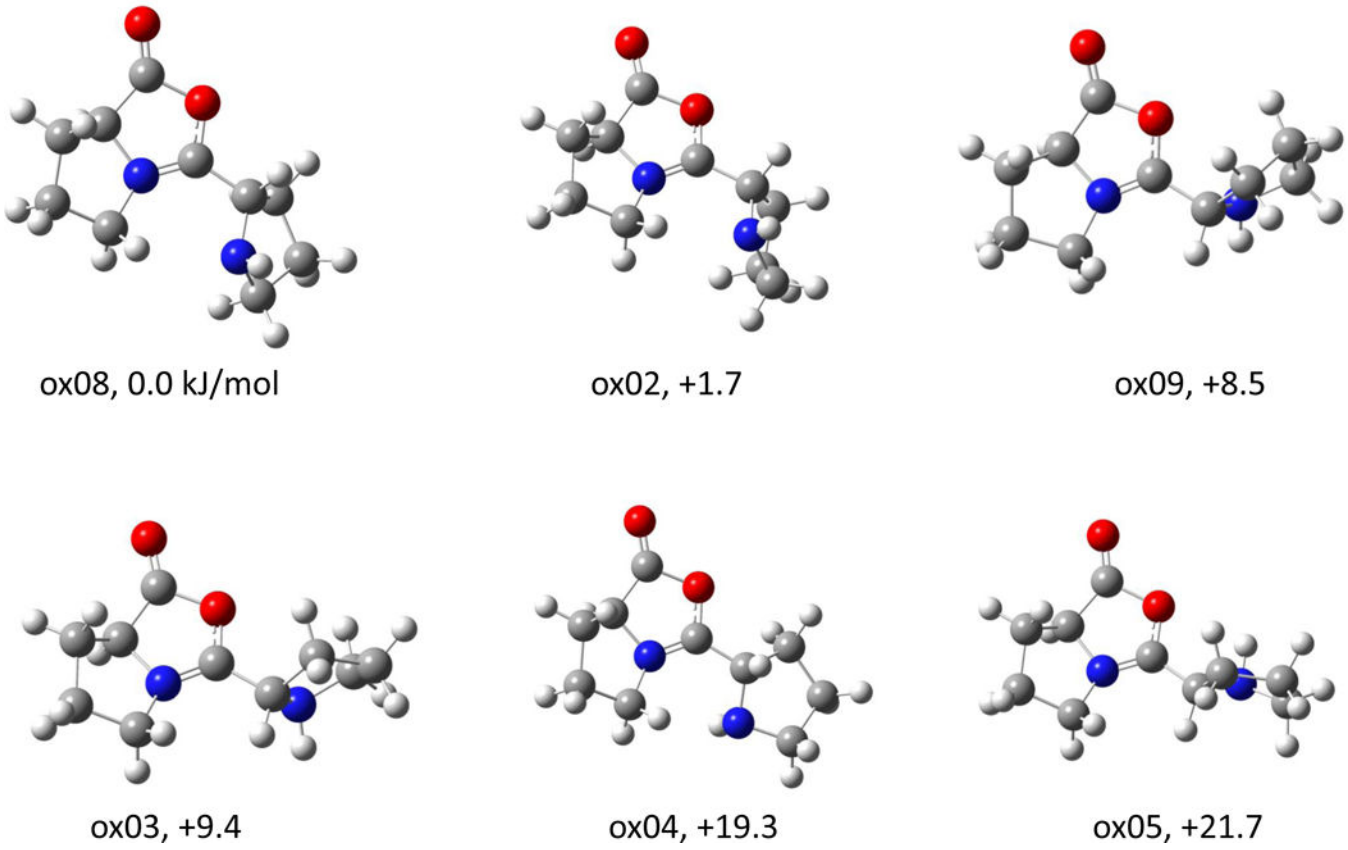

Figure 3.

Low-energy conformers for oxazolone PP b_2^+ ions. Numbers are ΔG values in kJ/mol at 298 K relative to the lowest energy oxazolone conformer, refer to Table S1 for ΔG values relative to the lowest energy diketopiperazine conformer.

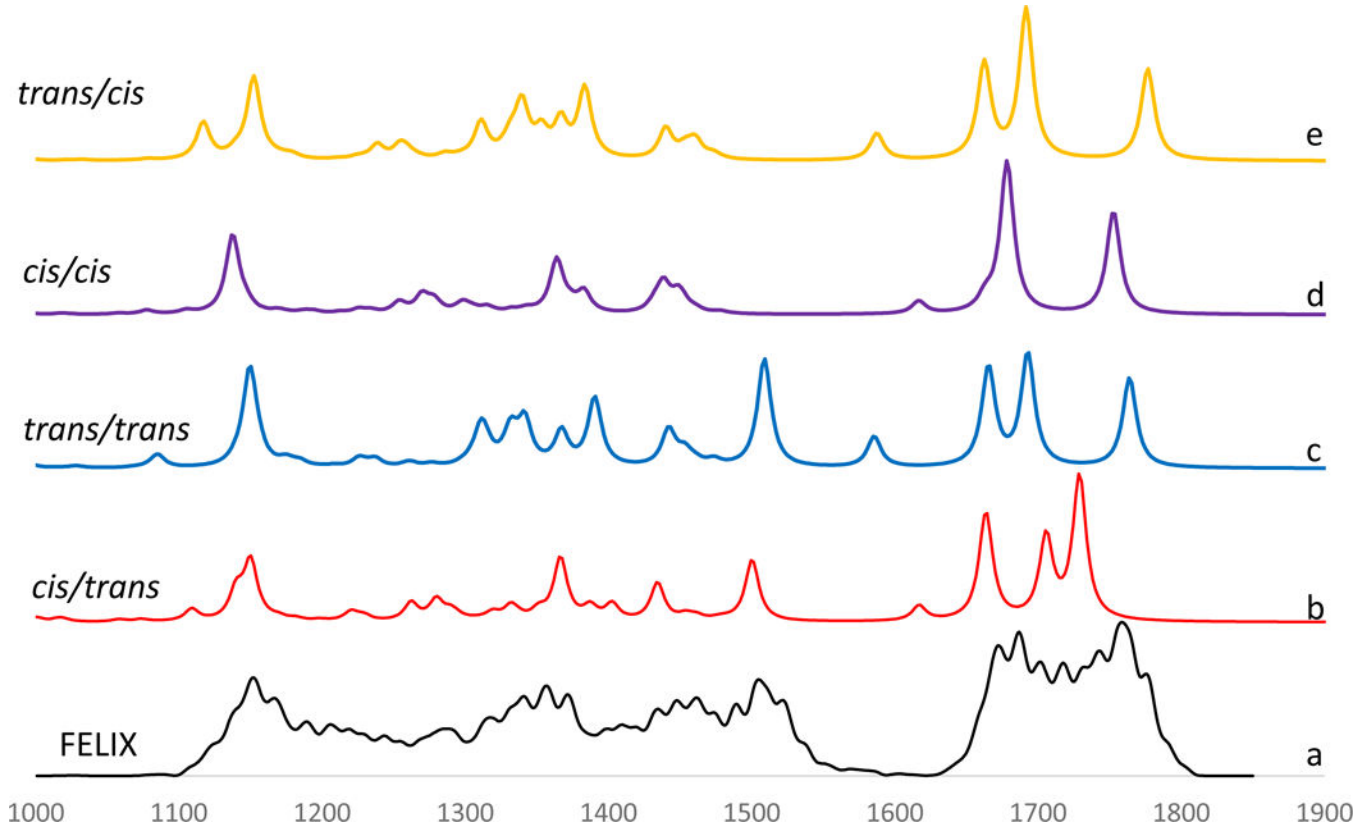

Figure 4.

a) Experimental IRMPD action spectrum for PPG+H^+ precursor ion obtained at a) FELIX. Computed spectra for the lowest energy b) *cis/trans* isomer, c) *trans/trans* isomer, d) *cis/cis* isomer, and e) *trans/cis* isomer of PPG+H^+.

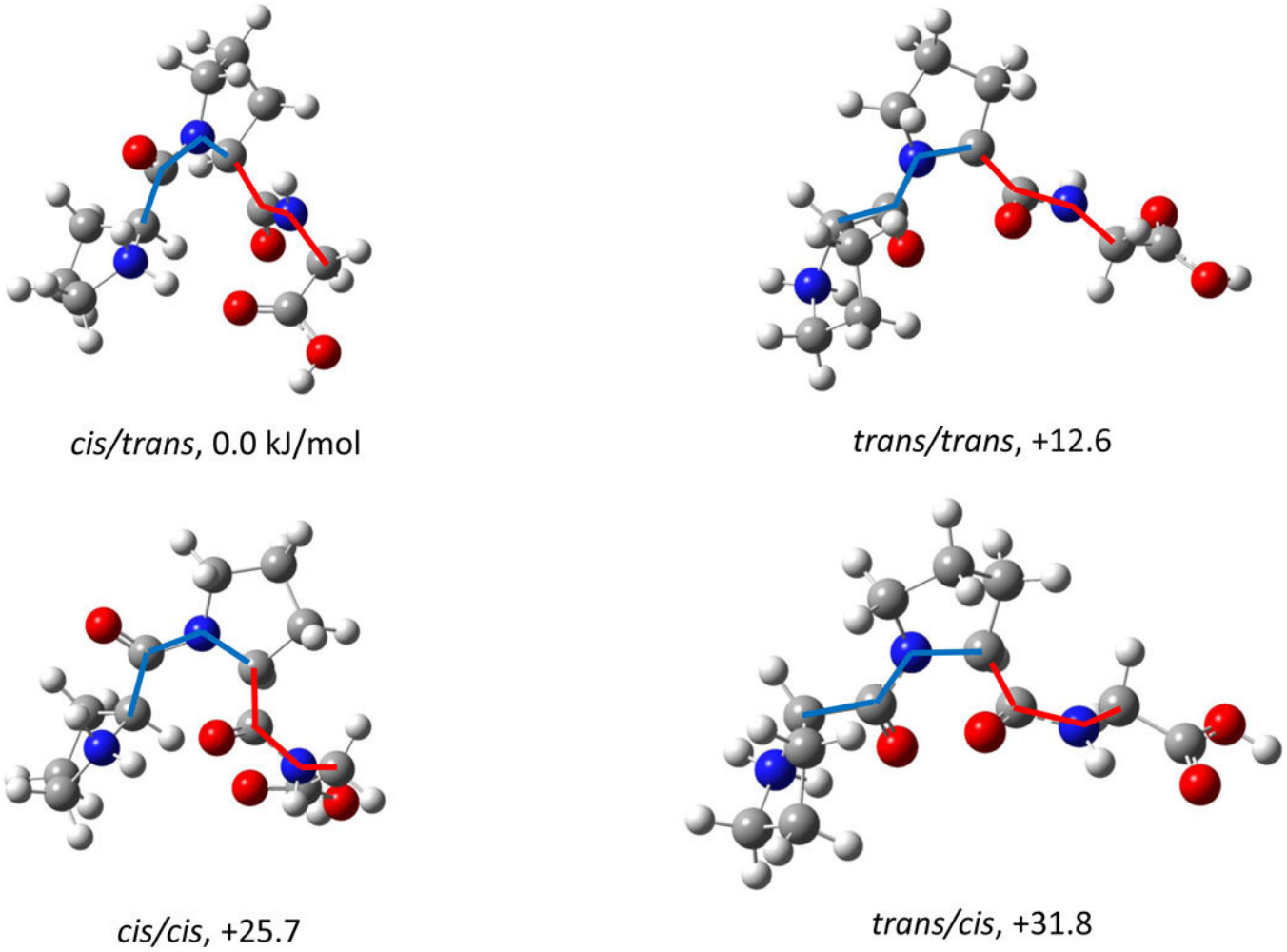

Figure 5.

Lowest-energy conformers for the a) *cis/trans* isomer, b) *trans/trans* isomer, c) *cis/cis* isomer, and d) *trans/cis* isomer of PPG+H^+. Numbers are ΔG values in kJ/mol at 298 K relative to the lowest energy conformer. Blue and red lines indicate the *cis/trans* configuration of the first and second peptide bonds.